Dyes and Pigments 88 (2010) 180–186

Contents lists available at ScienceDirect

Dyes and Pigments

journal homepage: www.elsevier.com/locate/dyepig

Thermal *cis*-to-*trans* isomerisation of triazene dyes in doped polymer films

Ryan Tabone, Mónica Barra*

Department of Chemistry, University of Waterloo, Waterloo, Ontario, Canada N2L 3G1

ARTICLE INFO

Article history:
Received 19 April 2010
Received in revised form
10 June 2010
Accepted 12 June 2010
Available online 25 June 2010

Keywords:
Photochromism
Triazenes
Z–*E* isomerisation
Kinetics
Doped films

ABSTRACT

The kinetics of the thermal conversion of the *cis* to the *trans* isomeric forms of 1,3-diphenyltriazene and 1-phenyltriazenes derived from cyclic amines were determined in both poly(methyl methacrylate) and polystyrene doped films in the glassy state, using UV–visible absorption spectroscopy. The kinetics of 1,3-diphenyltriazene are well explained by a two-exponential function, whilst those of 1-phenyltriazene derivates fit a first-order rate law. In all cases, the rate of thermal *cis*-to-*trans* isomerisation is higher in poly(methyl methacrylate) than in polystyrene. Rate dependence on dye structure and polymer matrix polarity is consistent with isomerisation taking place via a rotation mechanism.

© 2010 Elsevier Ltd. All rights reserved.

1. Introduction

Cis–*trans* (*Z*–*E*) isomerisation of double bonds, induced (at least in one direction) by exposure to light, constitute the foundation of a large number of photochromic compounds that are used in biosensors, molecular motors and shuttles, high-density data storage media and switching elements for microelectronics [1]. An interesting class of photoswitchable material based on *cis*–*trans* isomerisation around a nitrogen-nitrogen double bond is represented by triazenes, which have a diazoamino moiety (–N=N–N<) and offer potential use in light-driven molecular switches [2]. A rational design of triazene-based photoresponsive materials requires an understanding of the factors which control geometrical isomerisation mechanism(s) and reaction kinetics. In this context, previous studies by the present authors have focussed on the mechanism of thermal relaxation of photochemically generated *cis* isomeric forms of 1,3-diphenyltriazenes and of 1-phenyltriazenes derived from cyclic amines (i.e., trisubstituted triazenes) in homogenous solution. Thermally driven *cis*-to-*trans* isomerisation of 1,3-diphenyltriazenes dissolved in aqueous media involves an acid/base-promoted 1,3-prototropic rearrangement (Scheme 1) [3], analogous to acid/base-catalyzed keto-enolisation [4]; thermal *cis*-to-*trans* isomerisation of 1-phenyltriazenes derived from cyclic amines, in contrast, proceeds in organic solvents via an internal rotation mechanism (Scheme 2) involving heterolytic rupture of the N=N π-bond and twisting around the C–N=N–N dihedral angle [5], in a manner similar to the isomerisation of donor/acceptor-substituted ('push–pull') azobenzenes [6].

Bearing in mind that many applications of photoresponsive materials require the chromophores to be incorporated in a polymeric matrix of some sort, and since *cis*–*trans* isomerisation reactions are space-demanding processes (hence, one would expect isomerisation kinetics to be influenced by environment-imposed constrains), a study of the kinetics of thermal relaxation from *cis* to *trans* isomeric forms of 1,3-diphenyltriazene (DPT) and of a set of 1-phenyltriazenes derived from cyclic amines (Chart 1) was carried out in doped polymer films using poly(methyl methacrylate) (PMMA) and polystyrene (PS) of various M_w. The results of such a study are reported here.

2. Experimental

2.1. Materials

1,3-Diphenyltriazene (Aldrich) was purified by treatment with $Cd(OH)_2$ generated in situ from $Cd(NO_3)_2$ (Allied Chemical) in methanol (ACS grade, EM Science) basic aqueous solution, as described in the literature [7]. 1-Phenyltriazenes derived from cyclic amines were existing samples from a previous study [5]. Toluene (Omnisolv grade, EM Science) was used as received. Seven poly(methyl methacrylate) polymers were employed as received; from Aldrich, a syndiotactic/atactic/isotactic (59/37/4) sample with M_w = 350,000 (T_g = 122 °C) and an atactic sample with

---

* Corresponding author. Tel.: +1 519 888 4567x35948; fax: +1 519 746 0435.
E-mail address: mbarra@uwaterloo.ca (M. Barra).

0143-7208/$ – see front matter © 2010 Elsevier Ltd. All rights reserved.
doi:10.1016/j.dyepig.2010.06.006

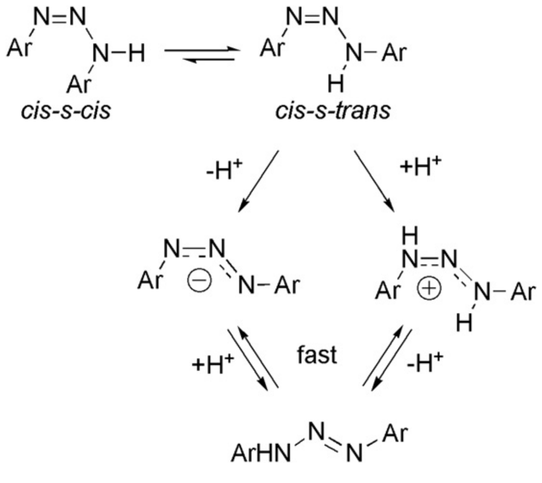

Scheme 1.

M_w = 996,000 (T_g = 125 °C); from Polymer Source, three atactic samples with M_w = 112,000 (M_w/M_n = 1.6), 226,000 (M_w/M_n = 1.9), and 641,000 (M_w/M_n = 2.0), respectively, and one syndiotactic/atactic/isotactic (79/16/5) sample with M_w = 114,500 (M_w/M_n = 1.08); from Scientific Polymer Products, an atactic sample with M_w = 75,000 (T_g = 98 °C). Three polystyrene polymers (from Polymer Source) were employed as received; atactic samples with M_w = 10,800 (M_w/M_n = 1.08), 51,000 (M_w/M_n = 1.06), and 310,300 (M_w/M_n = 1.1), respectively.

2.2. Methods

Polymeric films were prepared employing an extensor technique using solutions of PMMA (15 wt.%) or PS (10 wt.%) in toluene containing the triazene probe (DPT, ~1 mg/mL; trisubstituted triazenes, ~2 mg/mL). A small quantity of each viscous solution was dropped on a clean microscope slide and the solution was then extended along the slide using a calibrated drawdown rod (AP-JR 28 from Paul N. Gardner Company). After solvent evaporation at room temperature, polymeric films of *ca.* 18 μm of thickness were obtained. For trials in solution, quartz cells constructed of 7 × 7 mm Suprasil tubing were employed.

All samples were irradiated using a Rayonet photoreactor fitted with one RPR-3500 Å lamp. After an irradiation period of 30 s, samples were quickly transferred to a UV–visible spectrophotometer where kinetic traces corresponding to thermal *cis*-to-*trans* isomerisation were recorded by measuring the increase in absorbance (at 355 nm (DPT) or 325 nm (1-phenyltriazene derivatives)) as a function of time. Percent photolytic decomposition yields were calculated from the absorbance values recorded before lamp irradiation and after the thermal *cis*-to-*trans* isomerisation was completed. In no case did light exposure in the conventional spectrophotometer lead to any detectable photoisomerisation or decomposition.

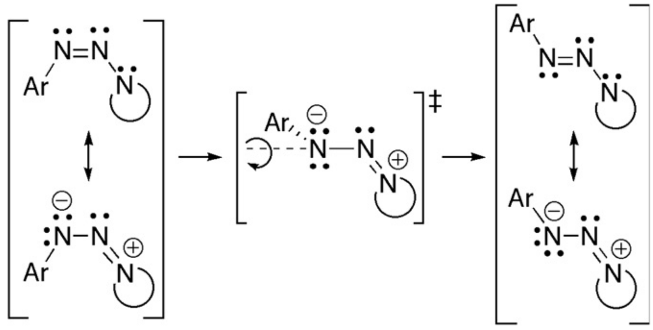

Scheme 2.

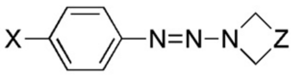

Substrate	X	Z
MeO-4	CH_3O	CH_2
MeO-5	CH_3O	$(CH_2)_2$
MeO-6	CH_3O	$(CH_2)_3$
MeO-6O	CH_3O	CH_2OCH_2
MeO-7	CH_3O	$(CH_2)_4$
Me-5	CH_3	$(CH_2)_2$
H-5	H	$(CH_2)_2$
H-6O	H	CH_2OCH_2
Cl-4	Cl	CH_2
CF_3-4	CF_3	CH_2
DPT	H	NHPh^a

^{a}In place of cyclic amino moiety

Chart 1. Target substrates.

All measurements were carried out at room temperature, i.e., (21 ± 1) °C, well below the glass transition temperature of the polymers employed in the study. Values for observed rate constants were obtained by fitting corresponding kinetic traces to single or double exponential functions using the general curve-fitting procedure of KaleidaGraph (version 3.6.4) from Synergy Software. Reported values correspond to the average of two to four independent runs. Lifetime distribution analyses were carried out using the exponential series method (ESM) software (modified version for transient absorption) from Photon Technology International. The fitting function consisted of 100 exponentials terms (with fixed, logarithmically spaced lifetimes ranging from 10 s to 10^6 s) and variable pre-exponential factors. Molecular modeling calculations were performed using the Gaussian03 package of programs [8], available at the facilities of the Shared Hierarchical Academic Research Computing Network (SHARCNET) and Compute/Calcul Canada. Full geometry optimizations were performed using DFT-B3LYP method and 6-31G* basis set. The characterization of stationary points was done as usual by Hessian matrix calculations; transition state structures were first located using the QST2 option.

3. Results and discussion

Target *cis*-triazenes were generated upon lamp irradiation (at 350 nm) of the corresponding *trans* form; the latter, as shown by X-ray diffraction measurements [9], appears to be the configuration always adopted in the ground-state. The embedding of target substrates in PMMA or PS films does not produce any relevant change in the absorption spectra of the *trans* isomers in comparison to the spectra recorded in organic solvents, indicating that photoexcitation (and in turn, photoisomerisation) of individual triazeno moieties in polymer matrices and in solution require essentially the same energy. Similar to the results reported for solution studies, *trans*-to-*cis* photoisomerisation of target substrates in doped polymer films leads to a decrease in absorbance around the λ_{max} of the longest wavelength absorption band (associated with the $\pi-\pi^*$ electronic transition of the triazeno group [10]), since *cis* isomers have lower absorptivity than the *trans* forms in that spectral region [3,5]. An increase in absorbance, however, takes place in the dark as the *cis* forms spontaneously isomerize back to the thermodynamically more stable *trans* isomers, as illustrated in Figs. 1 and 2 (the isosbestic points displayed at 310.5 and 359.6 nm, respectively, are certainly an indication of interconversion between two states).

Kinetic traces corresponding to thermal *cis*-to-*trans* isomerisation of DPT in doped PMMA or PS films in the glassy state cannot be fitted with a single exponential function, a common observation with photochromic unimolecular reactions taking place in constrained reaction media like polymer matrices [11]. Deviations from first-order kinetics are typically attributed to the inhomogeneous distribution of local free volume (sites) in the polymer matrix, hence imposing a distribution of localized barriers on the steric requirements of the reaction, as often reported for thermal *cis*-to-*trans* isomerisation of azobenzenes in polymer films [12], for example. Growth traces for thermal relaxation from *cis* to *trans* isomeric forms of DPT in doped films, however, are very well reproduced by a double exponential function (e.g., Fig. 1 inset), and resulting observed rate constants are summarized in Table 1. The applicability of a biexponential function agrees excellently with the results obtained from ESM analyses. As illustrated in Fig. 3 (top), EMS fittings reveal indeed a bimodal distribution both in PMMA and PS films, indicating at least two different modes of reaction (i.e., a ‘slow’ and a ‘fast’ isomerisation pathway). It is important to point out then that, since the kinetics in (DPT) doped polymer matrices seem to be controlled by distributions rather than by (two) discrete rate constants, the two values listed in Table 1 for each of the DPT samples analyzed represent empirical (mean) rate constants. Comparison of these values clearly indicates that, regardless of the polymer matrix employed, the slow thermal isomerisation mode (k_s), dominant in all cases, accounts for at least 70% (typically >80%) of the recovery signal, with k_s values in PS films being considerably smaller than those in PMMA films (a more polar matrix). Furthermore, changes neither in tacticity nor in molecular weight seem to have any significant influence on the rate of isomerisation, suggesting that, within the weight range employed in this study, there is no (significant) variation in free volume cavity size along the polymer series. It is also noticed that the reactivity in PMMA films (in agreement with an earlier report [13a]) is of comparable magnitude to that of the first-order rate constant for isomerisation in nonpolar solutions (e.g., 7×10^{-3} s^{-1} in cyclohexane [13b], 4×10^{-3} s^{-1} in benzene), which in turn is 10^6–10^8 times *lower* than that reported for DPT isomerisation in aqueous media [3a,3b].

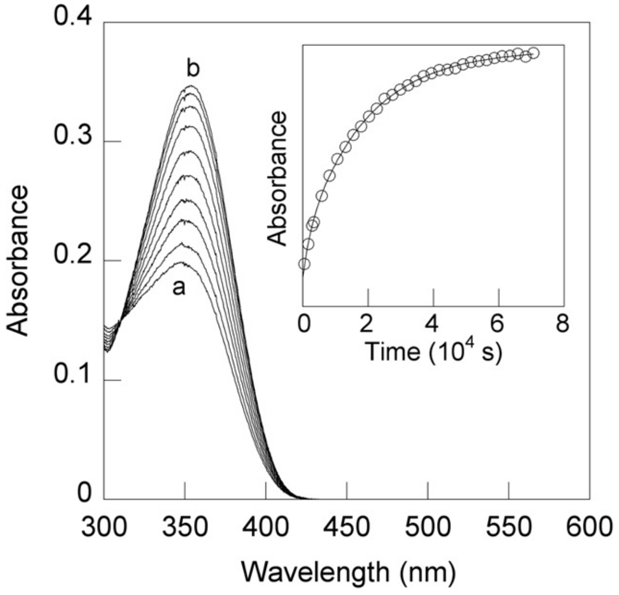

Fig. 1. Absorption spectra for DPT in PMMA film recorded within 10 s (a) and 1.5 h (b) after lamp irradiation. Inset: *cis*-to-*trans* kinetic trace for DPT in PS film. The solid line is the best fit to a biexponential function.

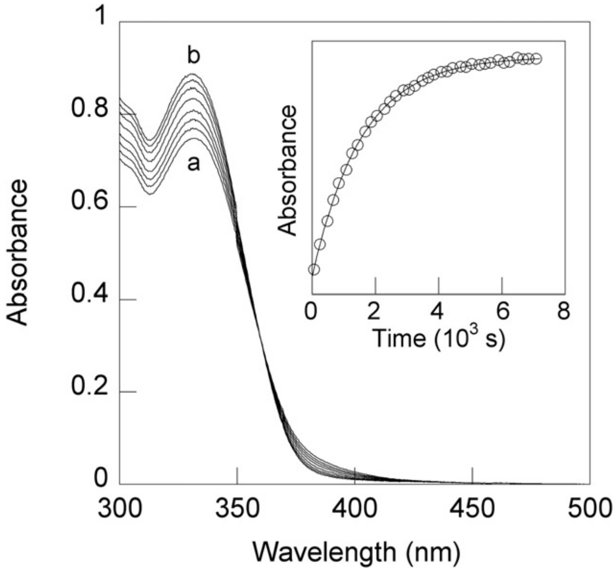

Fig. 2. Absorption spectra for Cl-4 in PMMA film recorded within 10 s (a) and 1.5 h (b) after lamp irradiation. Inset: corresponding *cis*-to-*trans* kinetic trace. The solid line is the best fit to a monoexponential function.

The isomerisation mechanism of DPT in aprotic solvents in the absence of proton carriers (i.e., under conditions where 1,3-prototropic rearrangements [14] are precluded [15]) is yet to be determined. Nevertheless, one may consider, similarly to the case of azobenzenes [6], the following two (limiting) mechanisms for thermal *cis*-to-*trans* isomerisation of DPT: a rotation mechanism (as illustrated in Scheme 2 for 1-phenyltriazene derivatives) or an inversion mechanism (via a transition state involving a linear sp hybridized nitrogen). Owing to the contribution of a 1,3-dipolar resonance form to the structure of the triazeno moiety ($-N^1{=}N^2{-}N^3{<} \leftrightarrow -N^-{-}N{=}N^+{<}$), which decreases the $N^1{=}N^2$ bond

Table 1
Observed rate constants for *cis*-to-*trans* isomerisation of DPT in doped polymer films[a].

Polymer[b]	M_w (g mol^{-1})	k_f (10^{-3} s^{-1})	k_s (10^{-3} s^{-1})	A_s[c] (%)
PMMA	75,000	5.3 (9)	1.1 (2)	92 (1)
	112,000	6 (1)	1.3 (1)	89 (3)
	114,500[d]	7.2 (8)	1.7 (1)	70 (5)
	226,000	5 (2)	1.4 (3)	75 (2)
	360,000[e]	4 (1)	0.84 (9)	87 (5)
	641,000	3.6 (1)	0.82 (1)	88 (1)
	996,000	4 (1)	1.1 (9)	80 (9)
PS	10,800	1.3 (6)	0.07 (2)	91 (2)
	51,000	0.7 (2)	0.05 (1)	87 (6)
	310,300	0.5 (2)	0.048 (6)	81 (9)

[a] Error for last significant figure given in brackets, $T = 21$ °C.
[b] Atactic polymer sample, unless stated otherwise.
[c] Percent pre-exponential (weight) factor for k_s.
[d] Syndiotactic/atactic/isotactic (79/16/5) polymer sample.
[e] Syndiotactic/atactic/isotactic (59/37/4) polymer sample.

order, one could expect triazenes to resemble the behavior of push–pull azobenzenes, hence predominance of a rotation mechanism would be anticipated. The 1,3-dipolar resonance form also accounts for the characteristic restricted rotation around the N^2–N^3 bond of *cis* [16] and *trans* [17] triazenes, which in turn leads to two minimum-energy conformations about the N–N bond (i.e., *s-cis* and *s-trans* rotamers) for each configurational isomer. Preliminary theoretical calculations for thermal *cis*-to-*trans* isomerisation of DPT in the gas phase render indeed transition state structures indicative of torsion around the N^1=N^2 bond (C-N=N-N *ca.* 90°) of the two minimum-energy *cis*-rotamers that are first generated (as non-equilibrium mixture) upon *trans*-to-*cis* photoisomerisation of DPT. As depicted in Fig. 4 and summarized in Table 2, the optimized transition states show, in comparison to the ground-state *cis* structures, not only torsion around the N=N group but also some degree of N^1 inversion, as inferred from the *ca.* 25° opening of the C–N=N angle and somewhat shortened N=N bond (in contrast to results for 1-phenyltriazenes, for which torsion around the N=N group is accompanied by lengthening of the N^1=N^2 bond [5], as expected for a simple rotation mechanism). One may speculate that the bimodal kinetics observed for thermal isomerisation of DPT in PMMA and PS doped films results from (a fraction of) the two metastable *cis*-rotamers (characterized by dissimilar isomerisation barriers due to stereoelectronic factors) not being able to interconvert freely in the polymer matrix. The non-monoexponential kinetics (typically modeled by a biexponentials function) for thermal *cis*-to-*trans* isomerisation of azobenzenes, for example, have been attributed to the trapping of some *cis* isomers in a stressed or strained state that isomerize more rapidly to the *trans* form than the relaxed-*cis* species (e.g., [12c,12e,12f]). Alternatively, since isomerisation of an azobenzene-PMMA copolymer has been shown not to influence the free volume cavity size of the

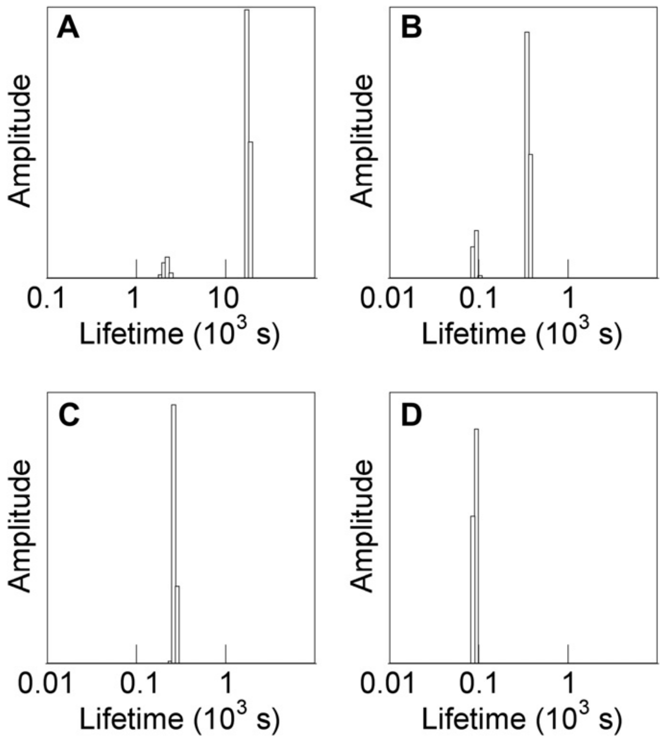

Fig. 3. Lifetime distributions for: (A) DPT in PS film, (B) DPT in PMMA film, (C) Me-5 in PS film, and (D) Me-5 in PMMA film.

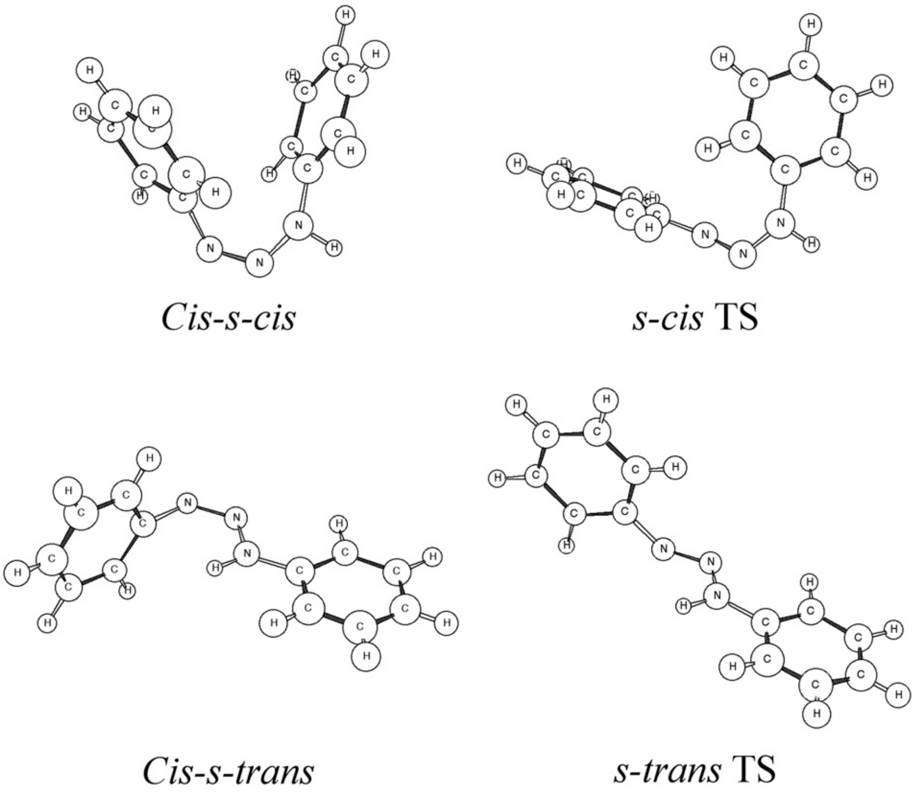

Fig. 4. Calculated lowest-energy *cis*-rotamers and corresponding transition state (TS) structures for thermal *cis*-to-*trans* isomerisation of DPT in the gas phase.

Table 2
Selected geometric parameters and energy barriers calculated for DPT in the gas phase at the B3LYP/6-31G* level of theory.

Parameter	Isomer					
	Cis-s-cis	*s-cis* TS[a]	*Trans-s-cis*	*Cis-s-trans*	*s-trans* TS[a]	*Trans-s-trans*
N=N (Å)	1.252	1.234	1.265	1.260	1.249	1.265
N–N (Å)	1.392	1.382	1.341	1.344	1.343	1.335
C–N=N (deg)	126.4	152.0	113.4	120.1	144.2	114.7
N=N–N (deg)	122.2	118.5	116.4	119.8	115.3	112.0
N–N–C (deg)	127.3	129.6	123.0	121.5	122.6	123.0
C–N=N–N (deg)	−7.4	−90.1	−180.0	−180.0	89.8	−180.0
Dipole (D)	3.240	3.425	1.535	3.252	4.019	0.921
ΔE^b (kcal mol^{-1})	20.3	39.5	4.6	9.4	36.7	0.0

[a] Transition state structure.
[b] Relative to *trans-s-trans* isomeric form, ZPE correction included.

copolymer, the bimodal kinetics for isomerisation of azobenzenes have been interpreted in terms of a four-state model, in which isomerisation only occurs in unrestricted sites whose occupancy is (in part) controlled by the rate of isomer exchange between restricted (unreactive) and unrestricted (reactive) sites [12b]. While these models certainly do not require multiple reacting isomeric species to rationalize non-monoexponential kinetics, we speculate the bimodal behavior observed for thermal isomerisation of DPT in PMMA and PS films derives from *cis*-rotamers relaxing to the *trans* form independently of each other, since kinetic traces corresponding to isomerisation of 1-phenyltriazenes involved in this study (i.e., triazenes with a symmetrically disubstituted N^3 site) fit to a monoexponential function (*vide infra*) regardless of guest size and reactivity order. Parallel reactions for (slow-interconverting) rotational isomers have indeed been reported not only for isomerisation of unsymmetrically substituted 1,3-diphenyltriazenes dissolved in aqueous media [3c,16b], but also for the ring closure reaction of carbamate derivatives [18], for instance. In regards to *cis*-DPT rotamers, it is noticed that for either conformational isomer an increase in dipole moment on going from ground-state *cis* structure to transition state is computed (Table 2), consistent with the increase observed both in k_f and k_s with increasing polymer matrix polarity (average values *ca.* 8×10^{-4} s^{-1} and 6×10^{-5} s^{-1} vs. 5×10^{-3} s^{-1} and 1×10^{-3} s^{-1} for k_f and k_s in PS and PMMA films, respectively).

Growth traces corresponding to thermal *cis*-to-*trans* isomerisation of target 1-phenyltriazenes derived from cyclic amines in doped PMMA or PS films in the glassy state, as just mentioned, are much simple. Kinetic traces are very well reproduced by a single exponential function (e.g., Fig. 2 inset), consistent with the unimodal distribution revealed by ESM analyses (Fig. 3, bottom); observed rate constants resulting from first-order fittings are summarized in Table 3. Comparison of values for PS (k_{PS}) or PMMA (k_{PMMA}) films clearly shows an increase in reactivity with (i) increasing cyclic amine ring size (MeO-4 to MeO-7), (ii) decreasing electronegativity of the cyclic amine ring atoms (MeO-6O vs. MeO-6), and (iii) increasing electronegativity of the phenyl ring substituent (e.g., MeO-4 < Cl-4 < CF$_3$-4). Moreover, for any given substrate, an increase in reactivity is seen on going from PS to PMMA films. Comparison of values given in Table 3 for Me-5 also indicates that neither tacticity nor polymer molecular weight, as in the case of DPT, seems to affect the isomerisation rate.

The rate dependence on photochromic dye structure and polymer matrix polarity described above for 1-phenyltriazenes derived from cyclic amines is in excellent agreement with the internal rotation mechanism (Scheme 2) previously proposed for thermal isomerisation in organic solvents [5], for which stabilization of a polar (charge-separated) transition state is crucial. The increase in reactivity observed with polymer polarity is certainly in agreement with matrix polarity effects reported for other polar photochromic

Table 3
Observed rate constants for *cis*-to-*trans* isomerisation of 1-phenyltriazenes derived from cyclic amines in doped polymer films[a].

Substrate	k_{PS}[b] (10^{-2} s^{-1})	k_{PMMA}[c] (10^{-2} s^{-1})
MeO-4	[d]	0.00026 (2)
MeO-5	0.065 (2)	0.211 (2)
MeO-6	1.41 (8)	3.2 (4)
MeO-6O	0.152 (2)	0.43 (1)
MeO-7	5.1 (4)	[d]
Me-5	0.442 (4)	1.22 (2)
	0.443 (5)[e]	1.10 (1)[f]
	0.436 (2)[g]	1.04 (2)[h]
		1.14 (1)[i]
H-5	2.03 (4)	6.0 (3)
H-6O	4.2 (2)	8 (1)
Cl-4	0.018 (1)	0.066 (2)
CF$_3$-4	0.79 (1)	5.0 (7)

[a] Error for last significant figure given in brackets, $T = 21$ °C.
[b] Atactic PS sample, $M_w = 51{,}000$ (unless stated otherwise).
[c] Syndiotactic/atactic/isotactic (59/37/4) PMMA sample, $M_w = 350{,}000$ (unless stated otherwise).
[d] Not measured.
[e] $M_w = 10{,}800$.
[f] Atactic PMMA sample, $M_w = 75{,}000$.
[g] $M_w = 310{,}300$.
[h] Atactic PMMA sample, $M_w = 226{,}000$.
[i] Atactic PMMA sample, $M_w = 641{,}000$.

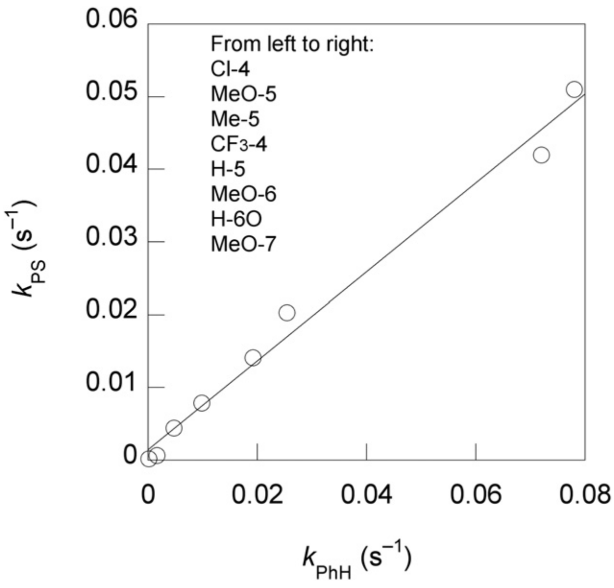

Fig. 5. Plot of observed rate constants for isomerisation of 1-phenyltriazene derivatives in polystyrene films versus reported values for isomerisation in benzene solution.

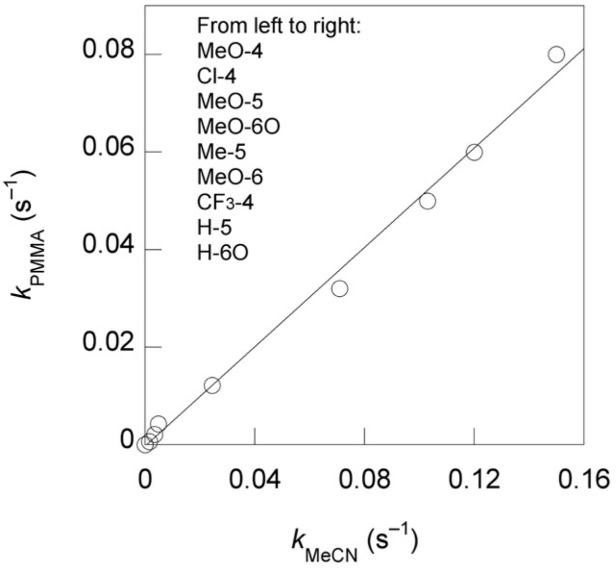

Fig. 6. Plot of observed rate constants for isomerisation of 1-phenyltriazene derivatives in poly(methyl methacrylate) films versus reported values for isomerisation in acetonitrile solution.

reactions, such as the electrocyclic ring opening characteristic of spiro-compounds, for example, whose rate increases in polar polymer matrices [19]. Interestingly, k_{PS} values are found to correlate very well with reported rate constants for isomerisation in benzene solution (Fig. 5), while k_{PMMA} values correlate excellently with those determined in acetonitrile solution (Fig. 6) [5]; slope values are 0.61 ± 0.03 and 0.51 ± 0.01, respectively (negligible intercept in both cases). These linear plots would be indicative of similar specific solute–solvent/polymer matrix interactions for each type of reaction medium, i.e., nonpolar (PS and benzene) or polar (PMMA and acetonitrile), as no linear correlation is in fact seen when comparing either k_{PS} vs. k_{PMMA} values or benzene vs. acetonitrile data.

Lastly, it is important to point out that under UV irradiation triazenes can not only undergo *trans*-to-*cis* photoisomerisation but also decompose via N^2–N^3 homolytic bond fission [20]. Photolysis easily manifests itself by an irreversible decrease in absorbance (bleaching) around the longest wavelength absorption band of triazenes; moreover, its yield is found to increase as the polarity of the reaction medium decreases [5,21], i.e., as the stabilization of the 1,3-dipolar resonance form of triazenes (*vide supra*), and hence the N^2–N^3 bond order, decreases.[1] Under the experimental conditions of this study, however, photolysis of target substrates is essentially negligible (typically <3%, if at all significant), even in the case of substrates for which decomposition in nonpolar solutions is certainly noticeable (e.g., 12% and 24%, respectively, for MeO-6 and MeO-6O [5] and 10% for DPT in benzene solutions). The decrease in photolytic decomposition in (nonpolar) polymer films relative to that in solution is attributed to a more effective in-cage radical-pair recombination (between phenylazenyl and amino/anilino radicals) in polymer matrices.

4. Conclusions

The rate of thermal *cis*-to-*trans* isomerisation of 1-phenyltriazenes derived from cyclic amines (i.e., trisubstituted triazenes) in doped PMMA and PS films in the glassy state can be described by a first-order rate law, whereas that for isomerisation of DPT (a disubstituted triazene) fits a biexponential function. Rate dependence on substrate structure (1-phenyltriazenes series) and on polymer matrix polarity (all substrates), in agreement with theoretical simulations (DPT) and previous solution studies (1-phenyltriazenes series), is consistent with geometrical isomerisation involving rotation around the $N{=}N$ bond via a dipolar transition state. In the case of 1-phenyltriazene derivatives, isomerisation rate constants determined in PMMA and PS films are found to be directly proportional to rate constants for isomerisation in acetonitrile and benzene solutions, respectively. Kinetic data presented herein should prove useful in the design of triazene-based photoresponsive materials.

Acknowledgments

We gratefully acknowledge partial funding from the Natural Sciences and Engineering Research Council (NSERC) of Canada.

References

[1] Dugave C, Demange L. Cis–trans isomerisation of organic molecules and biomolecules: implications and applications. Chem Rev 2003;103:2475–532.

[2] Zhao P, Zhang Z, Wang PJ, Liu DS. 1,3-Diphenyltriazene as a possible optical molecular switch: a first-principle study. Physica B 2009;404:3462–5.

[3] (a) Barra M, Chen N. Kinetic studies on the thermal cis–trans isomerisation of 1,3-diphenyltriazene in aqueous solution. Effects of acids and bases. J Org Chem 2000;65:5739–44;
(b) Chen N, Barra M, Lee I, Chahal N. Substituent effects on the thermal cis-to-trans isomerisation of 1,3-diphenyltriazenes in aqueous solution. J Org Chem 2002;67:2271–7;
(c) Zhang H, Barra M. Multiple-substituent effects on the isomerisation of unsymmetrical cis-1,3-diphenyltriazenes. J Phys Org Chem 2005;18:498–503.

[4] Keeffe JR, Kresge AJ. Kinetics and mechanism of enolization and ketonization. In: Rappoport Z, editor. The Chemistry of enols. New York: Wiley; 1990. p. 399–480.

[5] Fu J, Lau K, Barra M. Kinetic studies on the thermal cis-to-trans isomerisation of 1-phenyltriazenes derived from cyclic amines. J Org Chem 2009;74:1770–3.

[6] Knoll H. Photoisomerism of azobenzenes. In: Horspool WM, Lenci F, editors. CRC handbook of organic photochemistry and photobiology. Boca Raton: CRC Press; 2004. p. 89/1–89/16.

[7] Dwyer FP. A method of purification of diazoamino-compounds. J Chem Soc Ind London 1937;56:70–72T.

[8] Frisch MJ, Trucks GW, Schlegel HB, Scuseria GE, Robb MA, Cheeseman JR, et al. Gaussian 03, revision C.02. Wallingford: Gaussian, Inc.; 2004.

[9] (a) Hörner M, Visentin LC, Behm MB, Machado FC, Bortoluzzi AJ. Crystal structure of 1-(4-bromophenyl)-3-(4-nitrophenyl)triazene. Anal Sci 2007;23:x247–8;
(b) Karadayi N, Çakmak S, Odabaşoğlu M, Büyükgüngör O. 1,3-Bis(4-methylphenyl)triazene, 1-(4-chlorophenyl)-3-(4-fluorophenyl)triazene and 1-(4-fluorophenyl)-3-(4-methylphenyl)triazene. Acta Crystallogr 2005;C61:o303–5;
(c) Hörner M, Casagrande IC, Bordinhao J, Mössmer CM. 1,3-Bis(2,4-dibromophenyl)triazene. Acta Cryst 2002;C58:o193–4;
(d) Lunazzi L, Cerioni G, Foresti E, Macciantelli D. Conformational studies by dynamic nuclear magnetic resonance. Part X. Stereodynamics and conformations of hindered triazenes. J Chem Soc Perkin Trans 1978;2:686–91;
(e) Gladkova VF, Kondraskev YD. Crystal and molecular structures of diazoaminobenzene (β modification). Crystallogr Rep 1972;17:23–8.

[10] (a) Dabbagh HA, Teimouri A, Chermahini AN, Shiasi R. DFT and ab initio calculations of the vibrational frequencies and visible spectra of triazenes derived from cyclic amines. Spectrochim Acta, Part A 2007;67:437–43;
(b) Párkányi C, Vernin G, Julliard M, Metzger J. Electronic absorption and emission spectra of 1,3-diaryltriazenes. Helv Chim Acta 1981;64:171–5.

[11] Sworakowski J, Janus K, Nešpůrek S. Kinetics of photochromic reactions in condensed phases. Adv Colloid Interface Sci 2005;116:97–110.

[12] (a) Janus K, Sworakowski J. An approximate non-isothermal method to study kinetic processes controlled by a distribution of rate constants: the case of a photochromic azobenzene derivative dissolved in a polymer matrix. J Phys Chem B 2005;109:93–101;
(b) Algers J, Sperr P, Egger W, Liszkay L, Gottfried K, de Baerdemaeker J, et al.

---

[1] Predominant photolytic decomposition precluded indeed the analysis of *N*-substituted DPT derivatives such as 3-methyl-1,3-diphenyltriazene [22], to study further the role of unsymmetrical disubstitution at N^3 on the isomerisation mechanism.

Free volume determination of azobenzene-PMMA copolymer by a pulsed low-energy positron lifetime beam with in-situ UV illumination. Macromolecules 2004;37:8035–42;
(c) Wang C, Weiss RG. Thermal cis → trans isomerisation of covalently attached azobenzene groups in undrawn and drawn polyethylene films. Characterization and comparisons of occupied sites. Macromolecules 2003;36:3833–40;
(d) Janus K, Matczyszyn K, Sworakowski J, Biernat JF, Galewski Z. Kinetics of photochromic reactions of substituted azobenzenes in solutions, and in liquid crystalline and polymer matrices. Mol Cryst Liq Cryst 2001;361:143–8;
(e) Imai Y, Naka K, Chujo Y. Isomerisation behavior of azobenzene chromophores attached to the side chain of organic polymer in organic-inorganic polymer hybrids. Macromolecules 1999;32:1013–7;
(f) Barrett C, Natansohn A, Rochon P. Cis–trans thermal isomerisation rates of bound and doped azobenzenes in a series of polymers. Chem Mater 1995;7:899–903;
(g) Beltrame PL, Paglia ED, Castelli A, Tantardini GF, Seves A, Marcandalli B. Thermal cis–trans isomerisation of azo dyes in poly(methyl methacrylate) matrix: a kinetic study. J Appl Polym Sci 1993;49:2235–9.

[13] (a) Baro J, Dudek D, Luther K, Troe J. The photochemistry of 1,3-diphenyltriazene in various media. II: solid state photolysis. Ber Bunsenges Phys Chem 1983;87:1161–4;
(b) Baro J, Dudek D, Luther K, Troe J. The photochemistry of 1,3-diphenyltriazene in various media. I: photolysis in liquid solution. Ber Bunsenges Phys Chem 1983;87:1155–61.

[14] Scaiano JC, Chen C, McGarry PF. A flash photolysis and optoacoustic calorimetry study of the cis–trans isomerisation of 1,3-diphenyltriazene. J Photochem Photobiol A 1991;62:75–81.

[15] Männle F, Limbach HH. An intramolecular base-catalyzed proton transfer in 1,3-bis(4-fluorophenyl)triazene. Angew Chem Int Ed Engl 1996;35:441–2.

[16] (a) Barra M, Srivastava S, Brockman E. Substituent and solvent effects on the N2-N3 hindered rotation of cis-1,3-diphenyltriazenes. J Phys Org Chem 2004;17:1057–60;
(b) Barra M, Lim H. Structure-reactivity correlation study on the restricted rotation of cis-1,3-diphenyltriazenes. Trends Org Chem 2006;11:17–28.

[17] (a) Panitz JC, Lippert T, Wokaun A. Internal rotation of 1-aryl-3,3-dialkyltriazenes. Comparison of semiempirical molecular orbital calculations with Far-infrared, Raman, and NMR spectroscopic results. J Phys Chem 1994;98:8817–22;
(b) Lippert T, Wokaun A, Dauth J, Nuyken O. NMR studies of hindered rotation and thermal decomposition of novel 1-aryl-3,3-dialkyltriazenes. Magn Reson Chem 1992;30:1178–85;
(c) Foster N, Pestel B. Dynamic ^{13}C NMR: a study of aryl-substituted 1-phenyl-3,3-tetramethylenetriazenes. Magn Reson Chem 1985;23:83–5;
(d) Akhtar MH, McDaniel RS, Feser M, Oehlschlager AC. NMR study of hindered rotation in 1-aryl-3,3-dimethyltriazenes. Tetrahedron 1968;24:3899–966;
(f) Marullo NP, Mayfield CB, Wagener EH. Restricted rotation about the N–N single bond. Linear correlation of rate with substituent. J Am Chem Soc 1968;90:510–1.

[18] Hanusek J, Sedlák M, Jansa P, Štěrba V. Study of ring closure reaction of substituted phenyl *N*-(2-thiocarbamoylphenyl)carbamates catalysed by methoxy ion. J Phys Org Chem 2006;19:61–7.

[19] (a) Lee DK, Cha HG, Pal U, Kang YS. Kinetics of decolorization of spironaphthooxazine-doped photochromic polymer film. J Phys Chem B 2009;113:12923–7;
(b) Lin JS. Interaction between dispersed photochromic compound and polymer matrix. Eur Polym J 2003;39:1693–700;
(c) Such G, Evans RA, Yee LH, Davis TP. Factors influencing photochromism of spiro-compounds within polymer matrices. J Macromol Sci Part C Polym Rev 2003;C43:547–79.

[20] (a) Lippert T, Stebani J, Nuyken O, Stasko A, Wokaun A. Photolysis of 1-aryl-3,3-dialkyltriazenes. J Photochem Photobiol A 1994;78:139–48;
(b) Julliard M, Scelles M, Guillemonat A, Vernin G, Metzger J. The photochemical behaviour of bis aryl-1,3-triazenes. Tetrahedron Lett; 1977:375–8.

[21] Panitz JC, Lippert T, Stebani J, Nuyken O, Wokaun A. AM1 and PM3 semiempirical calculations on 1-aryl-3,3-diethyltriazenes. Correlation of bond orders with rotational barriers and quantum yields of photolysis. J Phys Chem 1993;97:5246–53.

[22] Chen N. Kinetic studies on the hydrolytic decomposition and thermal *cis*-to- *trans* isomerisation of aromatic triazenes in solution [M.Sc.]. Waterloo: University of Waterloo; 2000.